NATIONAL AERONAUTICS AND SPACE ADMINISTRATION

TECHNICAL MEMORANDUM X-411

SOME OBSERVATIONS OF BASE HEATING AT MACH 3.0 ON A SIMULATED MISSILE WITH A JP-4 - LIQUID-OXYGEN ROCKET*

By Nick E. Samanich, J. Calvin Lovell
and Donald O. Barnett

SUMMARY

A simulated missile with a 4000-pound-thrust JP-4 - liquid-oxygen rocket was used to investigate base heating at Mach 3.0 and a simulated pressure altitude of 72,000 feet. Combustion-chamber pressures were varied from 425 to 600 pounds per square inch absolute and oxidant-to-fuel ratios from 1.7 to 2.65. In some firings, the recirculation of oxygen from the external airstream in the base region resulted in ignition and sustained burning of the entrained fuel-rich exhaust gases. These fires occurred at oxidant-to-fuel ratios of 2.3 and higher and increased the gas temperature in the base region from about 1100° to 2600° R. In other cases, however, identical test conditions did not result in base fires. At oxidant-to-fuel ratios less than 2.3, no base fires were observed. With no base fire, maximum measured heat flux into the base was approximately 70 percent convective, the remainder radiant; during a fire, the base was heated almost entirely by convection (≈96 percent). Although the base- to ambient-pressure ratio varied with chamber pressure and oxidant-to-fuel ratio, the incremental increase accompanying the ignition and combustion of entrained exhaust gases was the same (≈0.1).

INTRODUCTION

In addition to radiation from the rocket jet, heat addition to the base region of rocket missiles can arise from the entrainment, recirculation, and combustion of exhaust gases. Actual base fires can occur when the fuel-rich exhaust gases combine with oxygen entrained from the external airstream. The result can be a substantial increase in the heat load on the base and any adjacent structures. Missile failures in flight caused by excessive temperatures in the base region have led to the initiation of base heating investigations at the Lewis Research Center. Various missile base geometries using single JP-4 - liquid-oxygen rockets have been studied at Mach numbers from 0.8 to 2.0 and

*Title, Unclassified.

simulated pressure altitudes from 8,500 to 36,000 feet (refs. 1, 2, and 3). In order to extend these studies to higher Mach numbers and altitudes, a simulated missile with a JP-4 - liquid-oxygen rocket was investigated in the Lewis 10- by 10-Foot Supersonic Wind Tunnel at a Mach number of 3.0 and a simulated pressure altitude of 72,000 feet. The model geometry was designed such that the external stream boundary intersected the rocket jet; a situation conducive to high heat loads in the base region, as shown in reference 2. Temperatures, heat flux, and pressures were measured in the base region during rocket operation at chamber pressures ranging from 425 to 600 pounds per square inch absolute and oxidant-to-fuel ratios from 1.7 to 2.65.

SYMBOLS

C^*	characteristic velocity, ft/sec
C_f	thrust coefficient
I	specific impulse, sec
o/f	oxidant-to-fuel weight ratio
P_c	combustion-chamber pressure, lb/sq in. abs
p	static pressure
p/p_0	ratio of local to free-stream static pressures
R	model body radius, 7.75 in.
r	radial location

Subscripts:

b	model base
e	nozzle exit

APPARATUS AND PROCEDURE

The tests were conducted in the Lewis 10- by 10-Foot Supersonic Wind Tunnel at a Mach number of 3.0 and a simulated pressure altitude of 72,000 feet.

Basic Model

A JP-4 - liquid-oxygen rocket was housed in a strut-supported $15\frac{1}{2}$-inch-diameter cone-cylinder body at zero angle of attack (fig. 1(a)). The rocket nozzle extended out 0.33 body diameter from the base and had an external exit diameter equal to 0.46 body diameter.

Rocket Motor

The rocket motor was rated at 4000-pounds thrust at a nominal chamber pressure of 600 pounds per square inch. The rocket nozzle (fig. 1(b)) had a 15°-half-angle conical expansion with an exit-to-throat area ratio of 8. A characteristic length of 50 inches and a combustion-chamber contraction ratio of 6.0 were used in the engine design. For the injector, like-on-like fuel impingement orifices and straight-through oxidant ports arranged in a showerhead design were used. A more detailed description of the motor and rocket system is given in reference 4.

Model Base and Instrumentation

The base, shown in figure 2, was a 3/8-inch-thick steel plate with approximately 1/8-inch clearance between it and the rocket motor. Firings were made with and without the base insulated with a 1/32-inch-thick zirconia coating (rokide "z").

Chromel-Alumel fast-response thermocouples of the design shown in figure 3(a) were used to measure gas temperatures in the base region. A number of thermocouples were located 3/4 inch out from the base at a radius ratio r/R of 0.82 (see fig. 2). Additional thermocouples were located circumferentially at the same radius but extended from 0 to $1\frac{1}{2}$ inches from the base surface to determine the extent of the thermal boundary layer. A thermocouple was also located inside the shell near the base plate to measure internal gas temperatures.

Two disk-type calorimeters (fig. 3(b)) were used to measure heat flux into the base region. Both were 0.032-inch-thick, 0.375-inch-diameter copper disks with a thermocouple embedded in the center. One disk was gold-plated, and the other was coated with lampblack suspended in a silicone varnish. These were located on the uninsulated base, 1/4 inch apart at $r/R = 0.82$ and symmetric with respect to the horizontal centerline (fig. 2).

All pressures were measured with transducers, and an electrical strain-gage balance was used to measure rocket thrust. Propellant weight flows were determined using rotating-vane-type flowmeters and measured propellant temperatures. All data were recorded automatically every 2.69 seconds except the disk temperatures, which were recorded continuously using photographic recording oscillographs.

RESULTS

Rocket Performance

Rocket performance parameters corrected to vacuum conditions are shown in figure 4 for a typical rocket firing. Steady-state conditions were maintained for approximately 25 seconds, with specific impulse, thrust coefficient, and characteristic velocity constant at values of 260 seconds, 1.7, and 5000 feet per second, respectively. Rocket firings were made at chamber pressures of 425 to 600 pounds per square inch absolute and oxidant-to-fuel ratios ranging from 1.7 to 2.65.

Base Heating

The maximum measured temperatures in the base region are presented in figure 5 as a function of the o/f ratio. All the temperatures are equilibrium values except for the one case where the gas temperature was still rising at the end of the firing. No corrections have been made for thermocouple radiation. During a number of firings, the entrained exhaust gases ignited and resulted in sustained base fires increasing the measured gas temperatures from about 1100° to about 2600° R. All the base fires (see fig. 5) occurred at the higher oxidant-to-fuel ratios ($\geq$ 2.3) but did not always reoccur under identical test conditions. This can be observed in three firings which were made under essentially the same operating conditions and resulted in entirely different temperature-time histories (see fig. 6). The three rocket firings were made at a chamber pressure of 600 pounds per square inch absolute and an oxidant-to-fuel ratio of approximately 2.6. Figure 6(a) is the time history of the gas temperatures at various distances from the base surface with no base fire. The maximum gas temperature was approximately 1100° R and was relatively constant during the firing. Figure 6(b) is a similar temperature-time history for a firing where the entrained exhaust gases ignited after about 17 seconds of steady-state rocket operation. In the third firing, a base fire occurred immediately upon rocket start with gas temperatures reaching steady values in approximately 7 seconds as shown in figure 6(c). In all instances where the entrained gases ignited, base burning was sustained until rocket shutdown. A tabulation of the test operating conditions for all the firings is presented in table I.

Temperature surveys indicated a 1/2-inch thermal boundary layer on the uninsulated base during all rocket firings. The variation of gas temperature with distance from the base at $r/R = 0.82$ is presented in figure 7 during representative firings with and without a base fire. Because of its large heat-sink capacity, the thick metal base plate kept the adjacent gas layer relatively cool with gas temperatures at the surface never exceeding 900° R, even when at 1/2 inch from the surface temperatures were on the order of 2500° R. Several firings with the base insulated with a 1/32-inch zirconia coating indicated a reduction in the thickness of the thermal boundary layer with maximum gas temperatures measured at distances as close as 1/4 inch from the surface. The effect of radial location on base gas temperatures was studied in reference 2 on a geometrically similar configuration at Mach 2.0 and indicated maximum gas temperatures occurred at radii between 0.55 and 0.85 of the base radius. An r/R of 0.82 was used in the present tests. Additional temperature surveys were made at various circumferential locations using thermocouples extending 3/4 inch from the base. The data indicated sustained but, to some degree, localized burning when the base fires occurred. This is shown in figure 8 where the circumferential temperature distributions in the base region are presented for two firings during a base fire of approximately 13-second duration. The nonuniformity in the temperature distribution and the fact that the points of extreme temperatures could shift circumferentially from one firing to the other indicate that the model strut support did not affect the distribution. The circumferential location of the areas of relative extreme temperatures, however, remained fixed during a given base-fire condition with differences as high as 1300° recorded.

Temperature data on a geometrically similar configuration at Mach 2.0 and a simulated pressure altitude of 36,000 feet are presented in reference 2. There, base fires were observed to occur at $o/f \geq 2.0$ with maximum gas temperatures of 1660° R. The difference between their results and those of the present study cannot be attributed solely to the change in Mach number and altitude. Other factors such as differences in combustion efficiencies, model size, nozzle contour, and thermocouple location also affect the comparison.

Heat flux measurements were limited to the initial rocket firing during each series of firings because of accumulating carbon deposits on the base. Measurements on the uninsulated base during two initial firings with a base fire were obtained and are subject to the previously mentioned qualifications of location and effects of local thermal boundary layer. The calorimeter-disk temperature-time histories for one of the firings with the ignition of the entrained gases occurring approximately $3\frac{1}{2}$ seconds after steady conditions were reached are presented in figure 9. For this firing, maximum gas temperature of about 1900° R was measured in the vicinity of the disks. Maximum total heat flux into the disks was calculated to be approximately 2 and 5 Btu per square foot per second without and with the base fire, respectively (see appendix for method of computation). The maximum heat flux measured was 70 percent convective, 30 percent radiant without the base fire, and 96 percent convective, 4 percent radiant with the base fire. These values are representative of both initial firings where reliable calorimeter data were available.

Base Pressures

Combustion-chamber, nozzle-exit static, and base pressures are presented in figure 10. The variation of nozzle-exit static pressure with combustion-chamber pressure is compared with theoretical values in figure 10(a) using references 5 and 6. The theory assumes complete combustion of the fuel in the combustion chamber with isentropic expansion assuming either frozen or equilibrium composition. In the present tests, however, combustion efficiency was approximately 88 percent. A linear increase of the base- to free-stream static-pressure ratio with nozzle-exit static-pressure ratio is evident in figure 10(b).

The base pressure and corresponding gas temperature for a specific firing (P_c = 525 lb/sq in. abs, o/f = 2.3) with a base fire occurring are presented in figure 11. After an initial aspiration of the base during starting propellant flows, the base- to ambient-pressure ratio increased from the value for rocket-off conditions (0.43) to about 0.80. As shown in figure 11, a further increase in p_b/p_0 of about 0.1 occurred with the onset of a base fire. This latter increment was representative of all cases where base fires were observed.

CONCLUDING REMARKS

A 4000-pound-thrust JP-4 - liquid-oxygen rocket housed in a cone-cylinder body was used to investigate base heating at Mach 3.0 and a simulated pressure altitude of 72,000 feet. Temperatures, heat flux, and pressures were measured in the base region at chamber pressures of 425 to 600 pounds per square inch absolute and oxidant-to-fuel ratios of 1.7 to 2.65. During some firings at oxidant-to-fuel ratios of 2.3 and higher, base fires occurred and increased the gas temperature in the base region from about 1100° to 2600° R. In other cases, however, identical test conditions did not result in base fires. At oxidant-to-fuel ratios less than 2.3, no base fires were observed. The maximum measured heat flux into the base was 70 percent convective, 30 percent radiant without a base fire, and was almost all convective during a base fire (96 percent).

Lewis Research Center
National Aeronautics and Space Administration
Cleveland, Ohio, August 8, 1960

[redacted]

APPENDIX - METHOD OF CALCULATION OF HEAT FLUX

(1) $q_b = \alpha_b q_r + q_c = \rho \delta C_p \left(\frac{dT}{d\theta}\right)_b$

(2) $q_g = \alpha_g q_r + q_c = \rho \delta C_p \left(\frac{dT}{d\theta}\right)_g$

Solving for q_r from (1) and (2):

(3) $q_r = \frac{q_b - q_g}{\alpha_b - \alpha_g}$

Rearranging 1:

(4) $q_c = q_b - \alpha_b q_r$

where

C_p disk specific heat, Btu/(lb)($^\circ$F) (see following table)

q_b total unit heat rate to black-faced disk, Btu/(ft^2)(sec)

q_c convective component of disk heat input, Btu/(ft^2)(sec)

q_g total unit heat rate to gold-faced disk, Btu/(ft^2)(sec)

q_r radiative component to perfect black body at the area under study, Btu/(ft^2)(sec)

$\frac{dT}{d\theta}$ temperature derivative at time in question

α_b absorbtivity of the black-faced disk, 0.73

α_g absorbtivity of the gold-faced disk, 0.07

δ disk thickness, 0.00266 ft

ρ disk density, 556.9 lb/cu ft

Temperature, $^\circ$F	C_p, Btu/(lb)($^\circ$F)
32	0.094
200	.095
400	.096
600	.099
800	.100
1000	.105
1200	.108

REFERENCES

1. Nettles, J. Cary: Experimental Study of Ballistic-Missile Base Heating with Operating Rocket. NACA RM E58G17, 1958.

2. Chiccine, Bruce G., Valerino, Alfred S., and Shinn, Arthur M.: Experimental Investigation of Base Heating and Rocket Hinge Moments for a Simulated Missile Through a Mach Number Range of 0.8 to 2.0. NASA TM X-82, 1959.

3. Valerino, Alfred S., Shinn, Arthur M., Jr., and Chiccine, Bruce G.: Effects of Base Bleed Flow on Base Region Temperatures and Pressures of Several Simulated Missile Afterbody Configurations - Mach Number Range of 0.8 to 2.0. NASA TM X-153, 1960.

4. Lovell, J. Calvin, Samanich, Nick E., and Barnett, Donald O.: Experimental Performance of Area Ratio 200, 25, and 8 Nozzles on JP-4 Fuel and Liquid-Oxygen Rocket Engine. NASA TM X-382, 1960.

5. Huff, Vearl N., and Fortini, Anthony: Theoretical Performance of JP-4 Fuel and Liquid Oxygen as a Rocket Propellant. I - Frozen Composition. NACA RM E56A27, 1956.

6. Huff, Vearl N., Fortini, Anthony, and Gordon, Sanford: Theoretical Performance of JP-4 Fuel and Liquid Oxygen as a Rocket Propellant. II - Equilibrium Composition. NACA RM E56D23, 1956.

E-912

E-912

CP-2

TABLE I. - CONDITIONS AT WHICH ROCKET FIRINGS WERE MADE

Oxidant-to-fuel ratio, o/f	Combustion-chamber pressure, P_c, lb/sq in. abs	Number of firings	Base fire
1.70	510	2	No
1.75	520	1	No
1.80	520	2	No
1.90	515	1	No
2.00	510	1	No
2.00	520	1	No
2.00	600	1	No
2.05	520	1	No
2.10	425	1	No
2.10	520	1	No
2.20	515	1	No
2.20	590	1	No
2.20	600	1	No
2.30	505	1	No
2.30	520	1	No
2.30	525	1	Yes
2.40	520	1	No
2.40	590	1	No
2.40	600	1	No
2.50	425	1	No
2.50	465	1	No
2.50	520	1	Yes
2.50	535	1	No
2.55	515	1	Yes
2.55	520	1	No
2.55	600	1	Yes
2.60	600	1	No
2.65	600	1	Yes

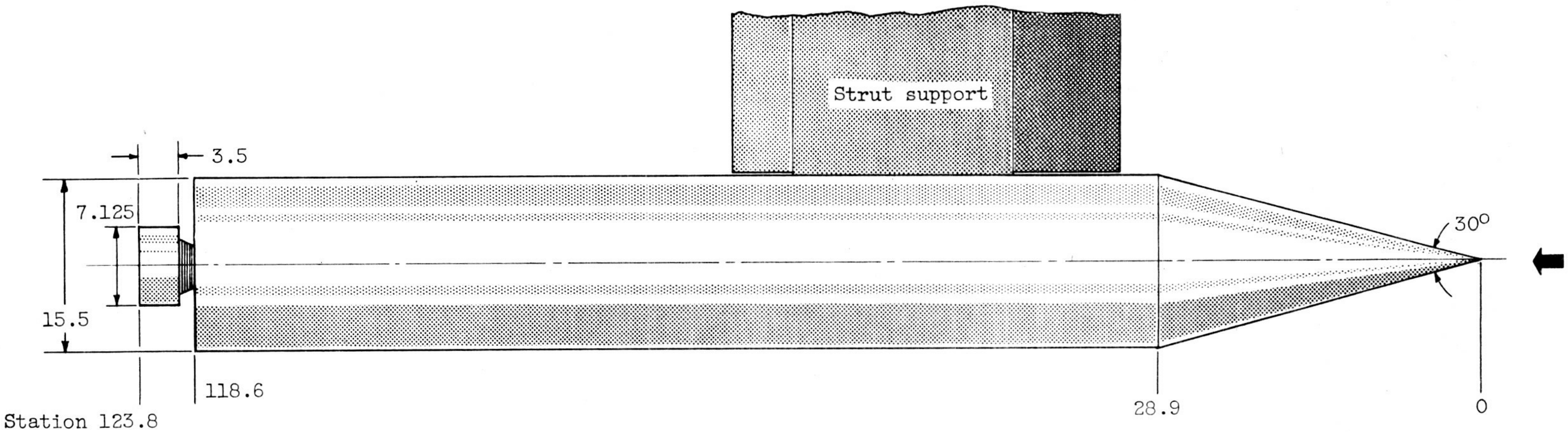

(a) Cone-cylinder body.

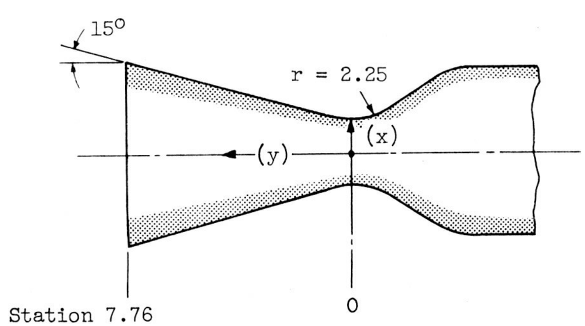

Coordinates	
y	x
0	1.103
(15°-half-angle conical taper to exit)	
7.76	3.11

CD-6952

(b) Internal nozzle contour (exit-to-throat area ratio = 8).

Figure 1. - Rocket model tested. (All dimensions in inches except where noted).

Thermocouple locations					
Station, deg	Distance from base, in.	Station, deg	Distance from base, in.	Station, deg	Distance from base, in.
5	3/4	206	1/16	242	3/4
35	3/4	212	1/8	248	1.0
100	3/4	218	3/16	254	1-1/2
135	3/4	224	1/4	290	3/4
185	3/4	230	3/8	315	3/4
200	0	236	1/2		

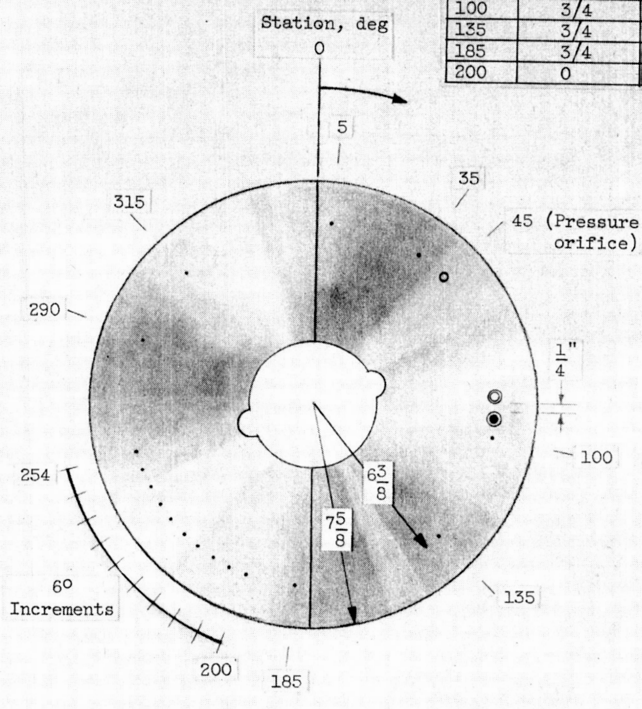

Instrumented base plate

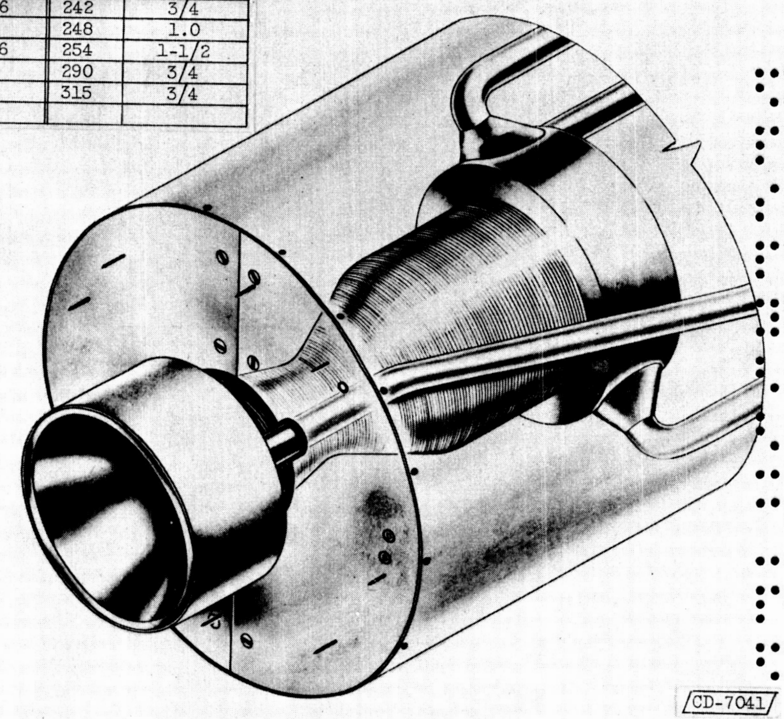

Three-quarter rear view of model base

Figure 2. - Base region of rocket model.

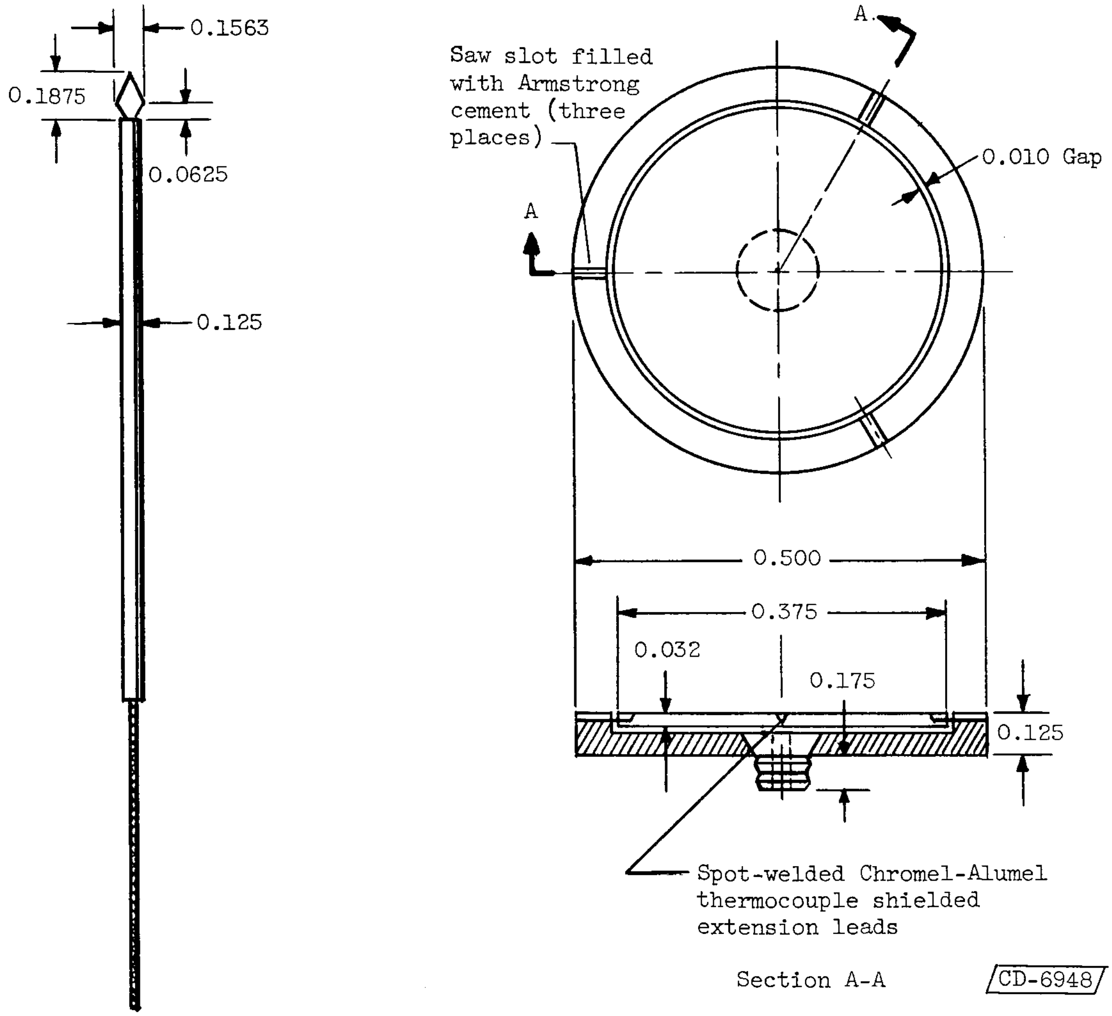

(a) Chromel-Alumel thermocouple (24-gage wire).

(b) Disk-type calorimeter.

Figure 3. - Details of thermocouple and calorimeter disk designs. (All dimensions in inches.)

[redacted]

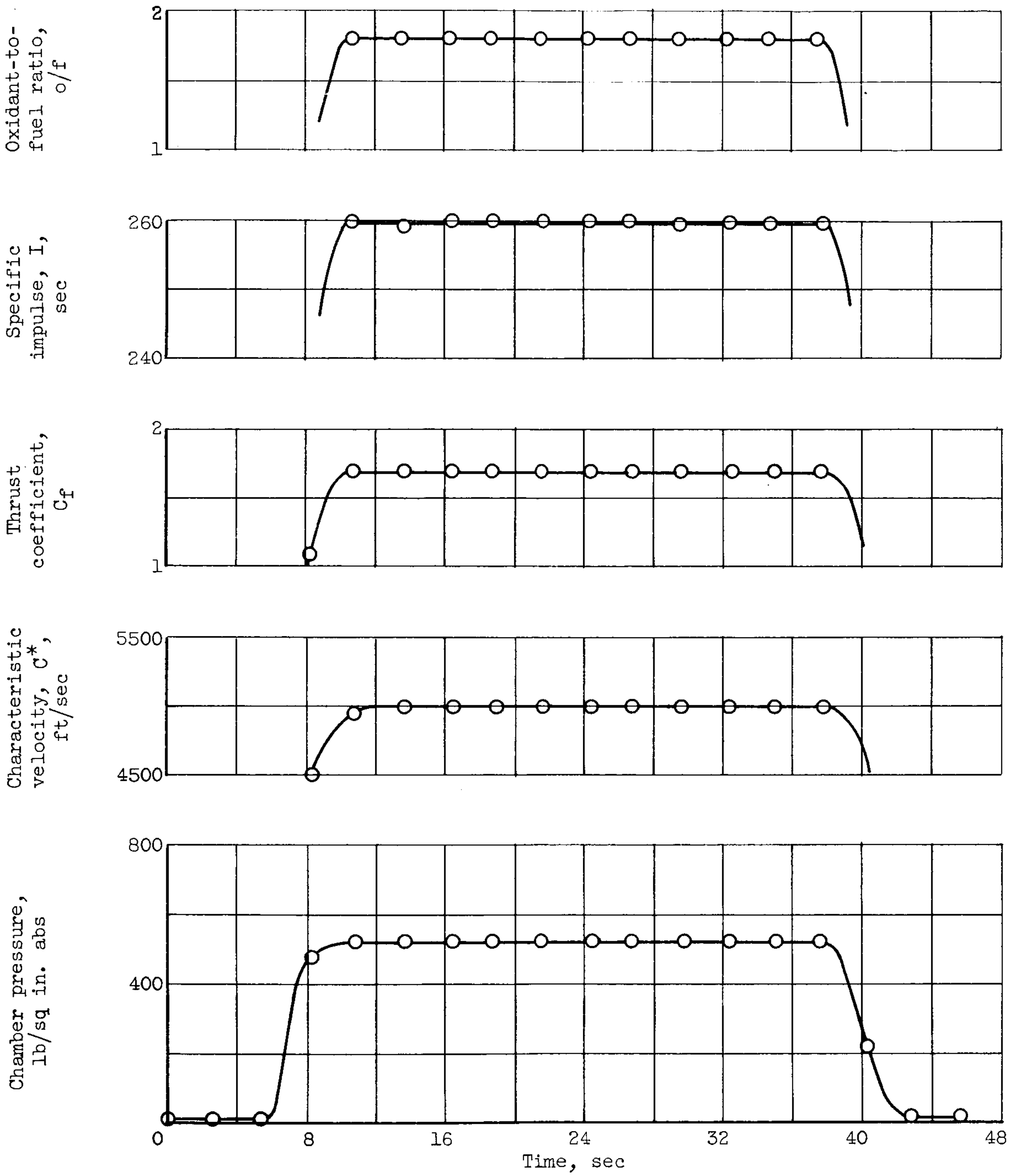

Figure 4. - Performance during typical rocket firing corrected to vacuum conditions.

[redacted]

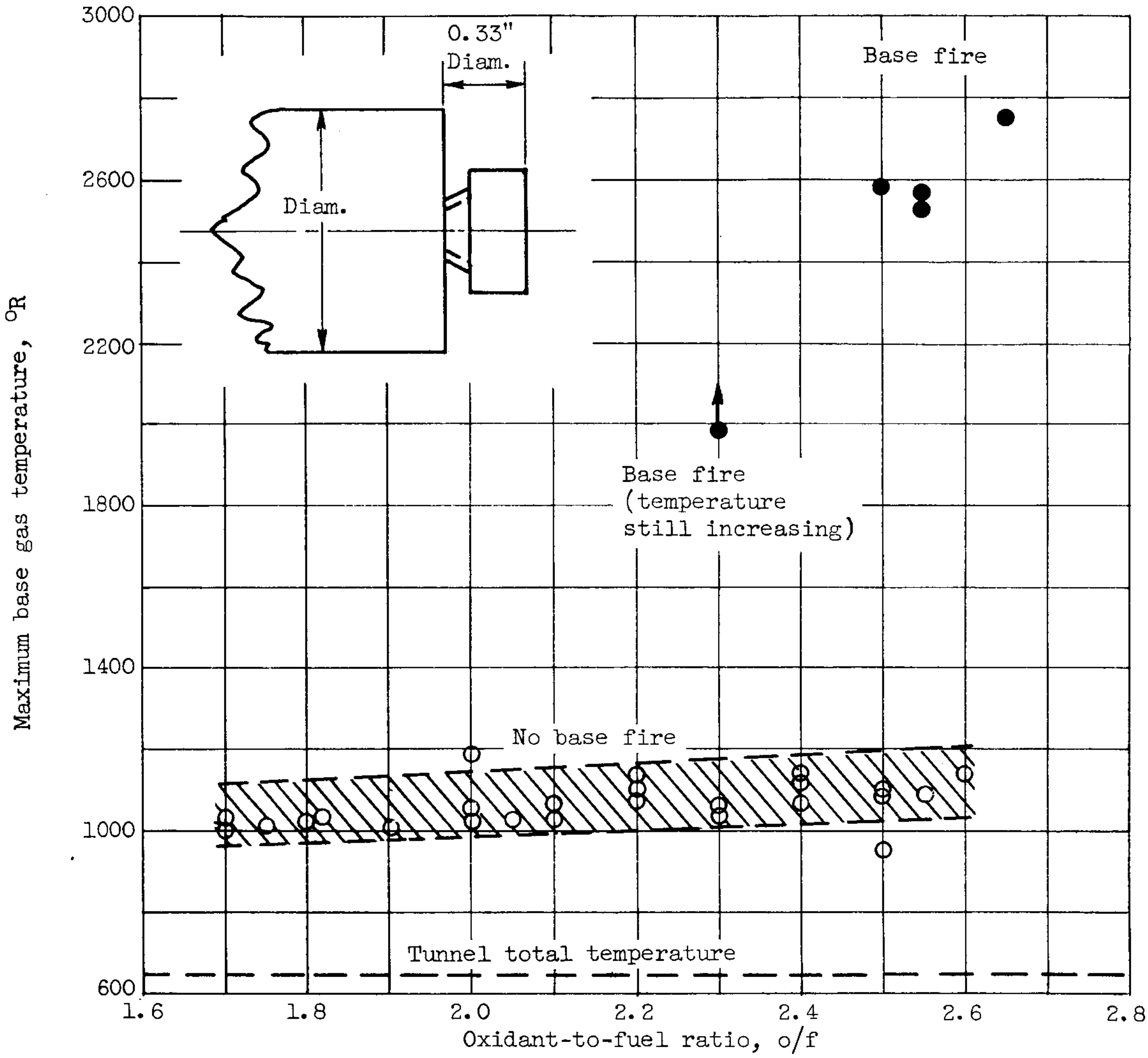

Figure 5. - Maximum gas temperature measured in base region as function of oxidant-to-fuel ratio. Characteristic velocity, 5000 feet per second; combustion-chamber pressure, 425 to 600 pounds per square inch absolute.

[redacted]

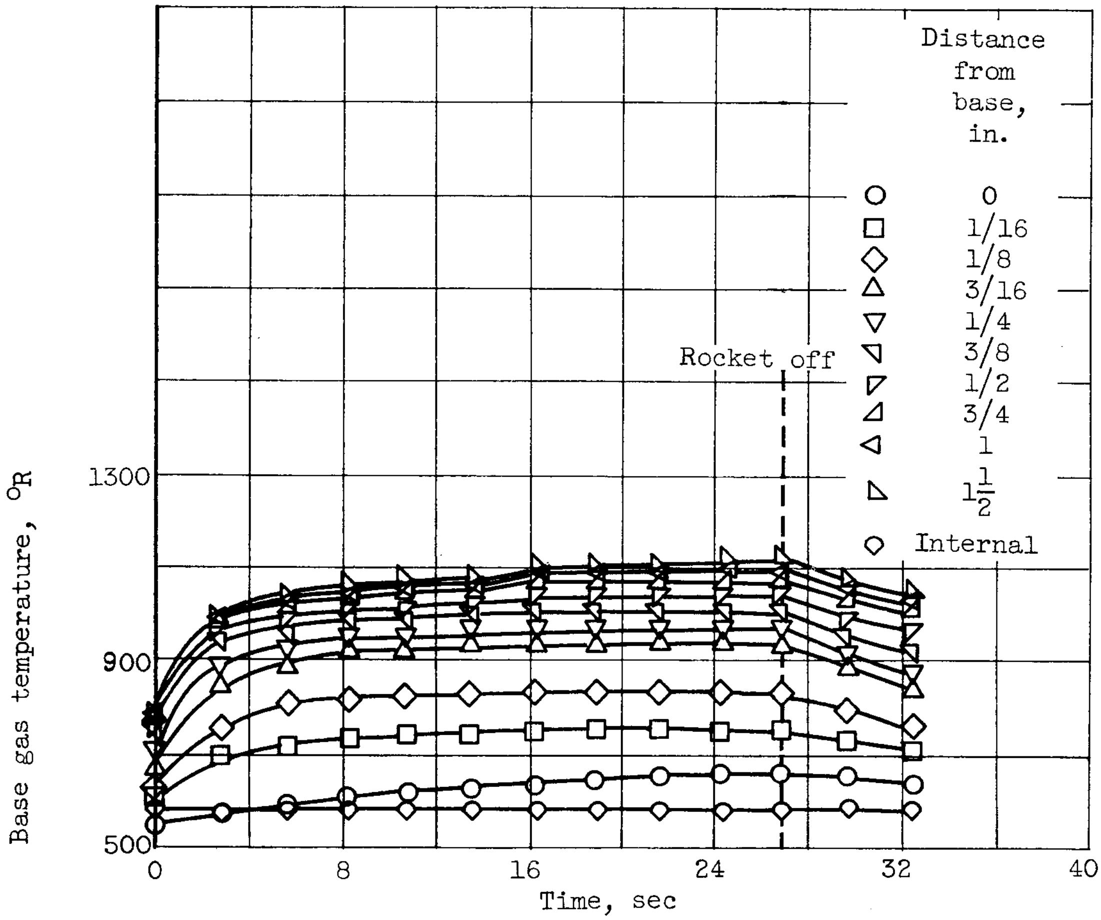

(a) No base fire.

Figure 6. - Base gas temperature at various distances out from base as function of time. Combustion-chamber pressure, 600 pounds per square inch absolute; oxidant-to-fuel ratio, ≈ 2.6.

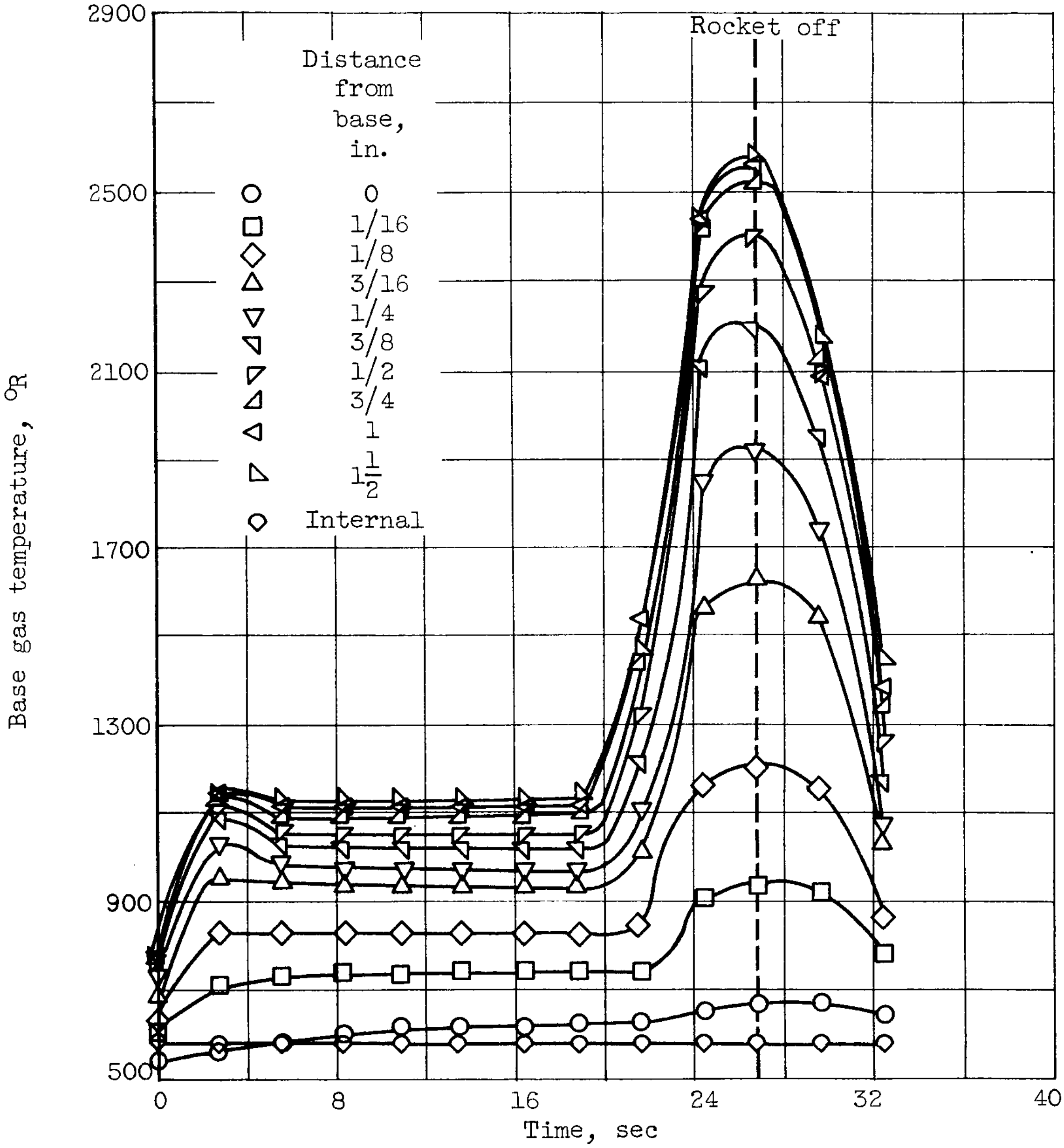

(b) Base fire near end of rocket firing.

Figure 6. - Continued. Base gas temperature at various distances out from base as function of time. Combustion-chamber pressure, 600 pounds per square inch absolute; oxidant-to-fuel ratio, ≈ 2.6.

[redacted]

E-912

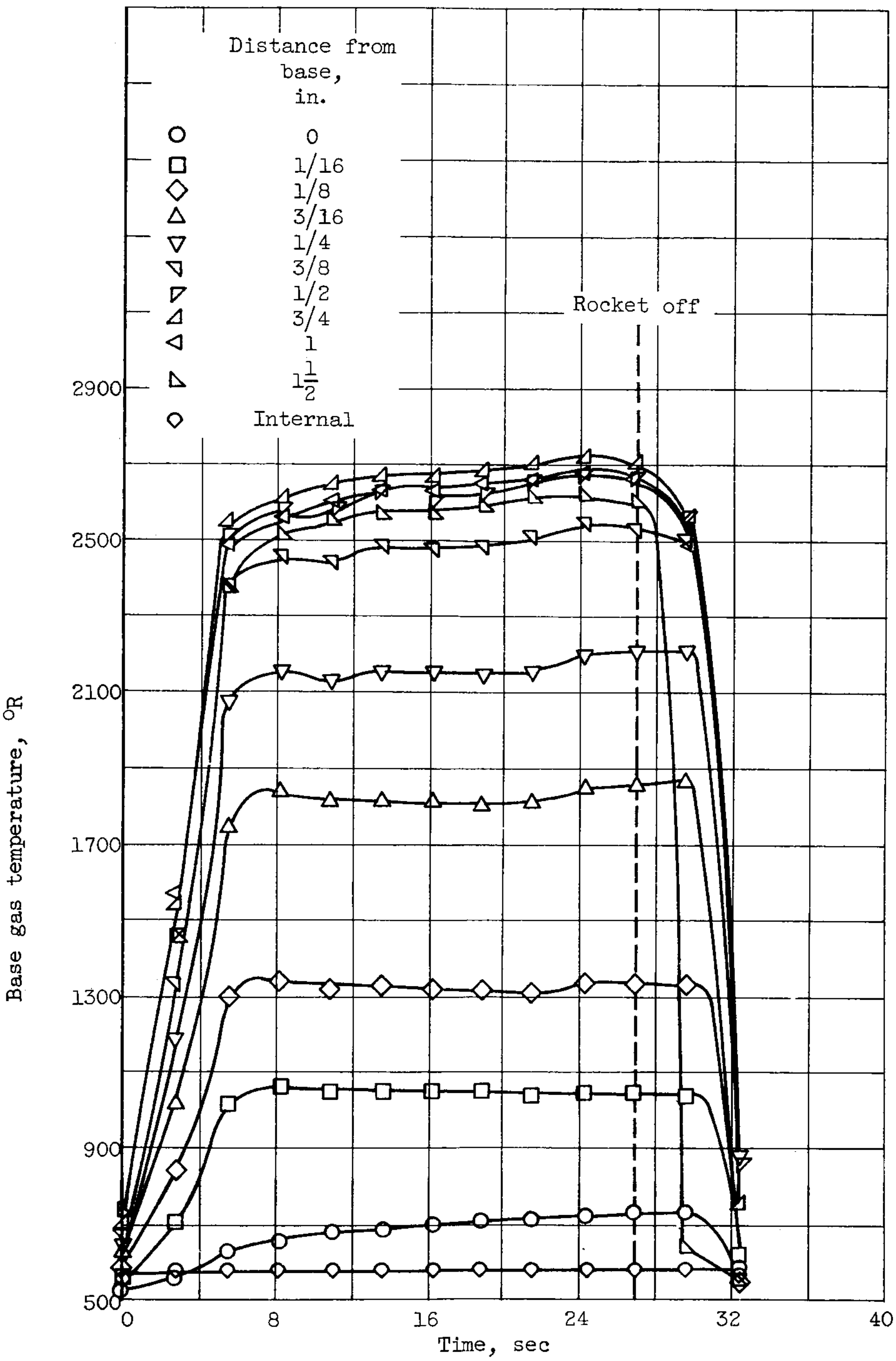

(c) Base fire during entire rocket firing.

Figure 6. - Concluded. Base gas temperature at various distances out from base as function of time. Combustion-chamber pressure, 600 pounds per square inch absolute; oxidant-to-fuel ratio, ≈ 2.6.

[redacted]

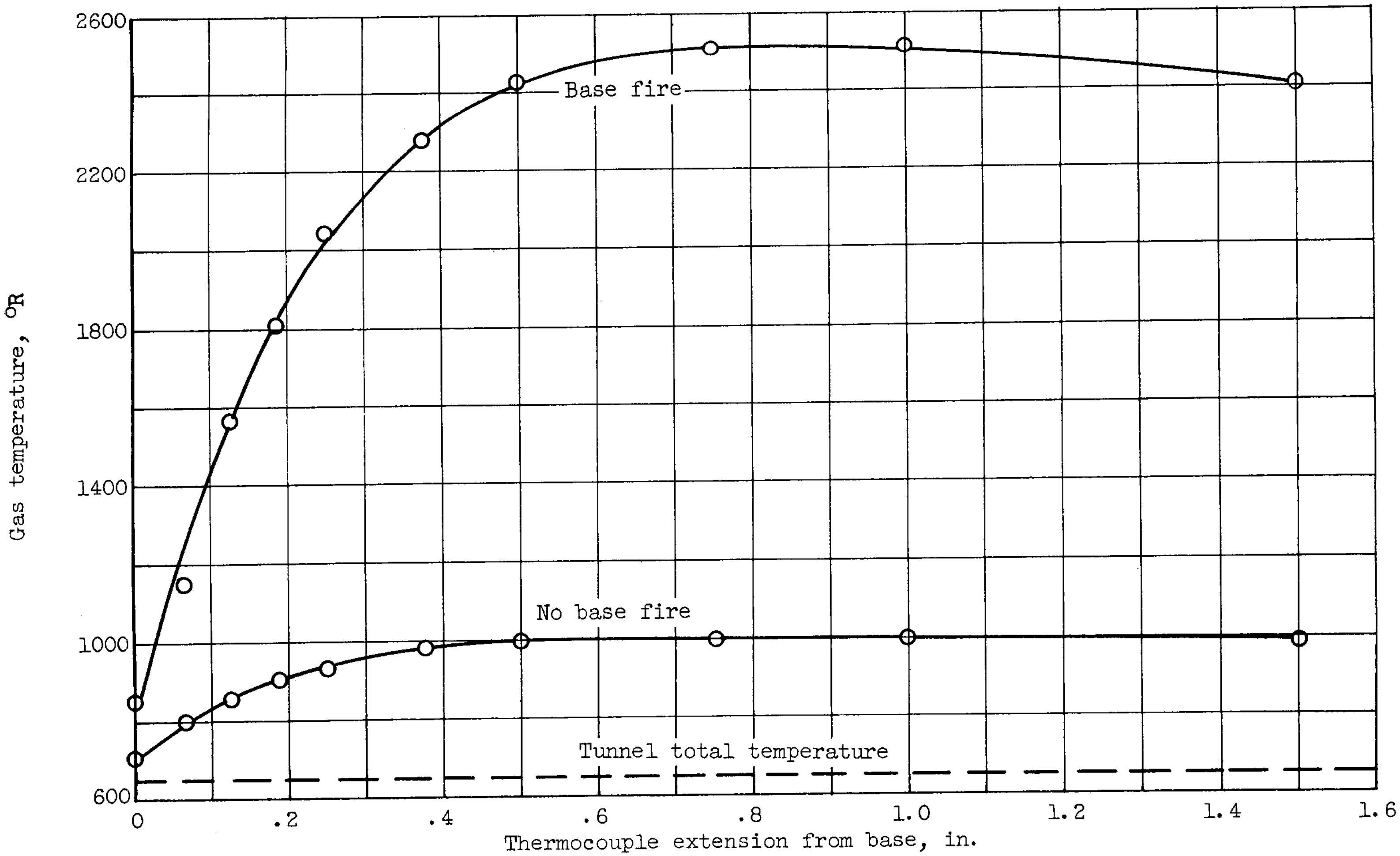

Figure 7. - Equilibrium gas temperatures at various distances from base with and without base fire.

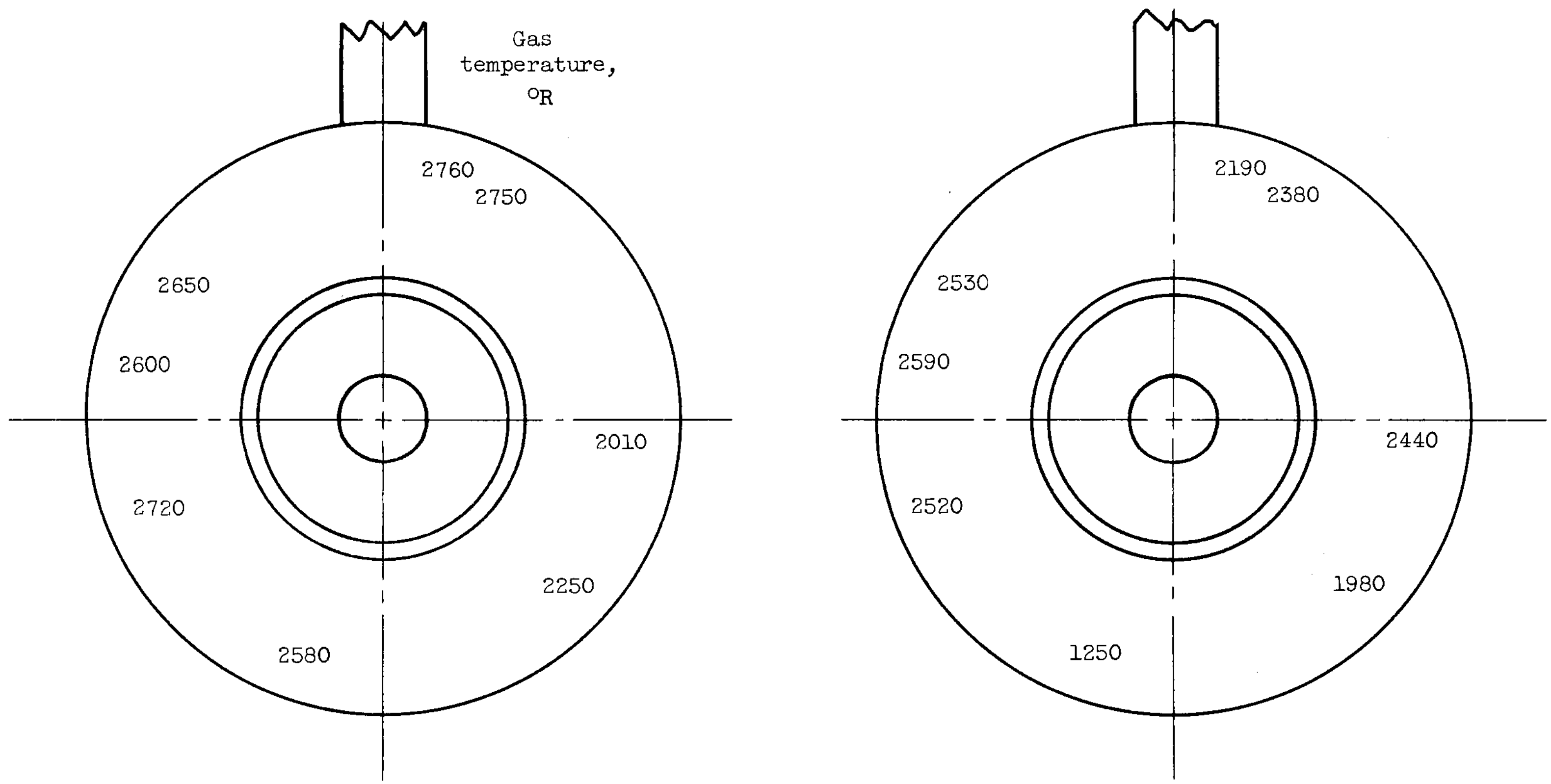

Figure 8. - Equilibrium gas temperatures 3/4 inch from base during two firings with base fire.

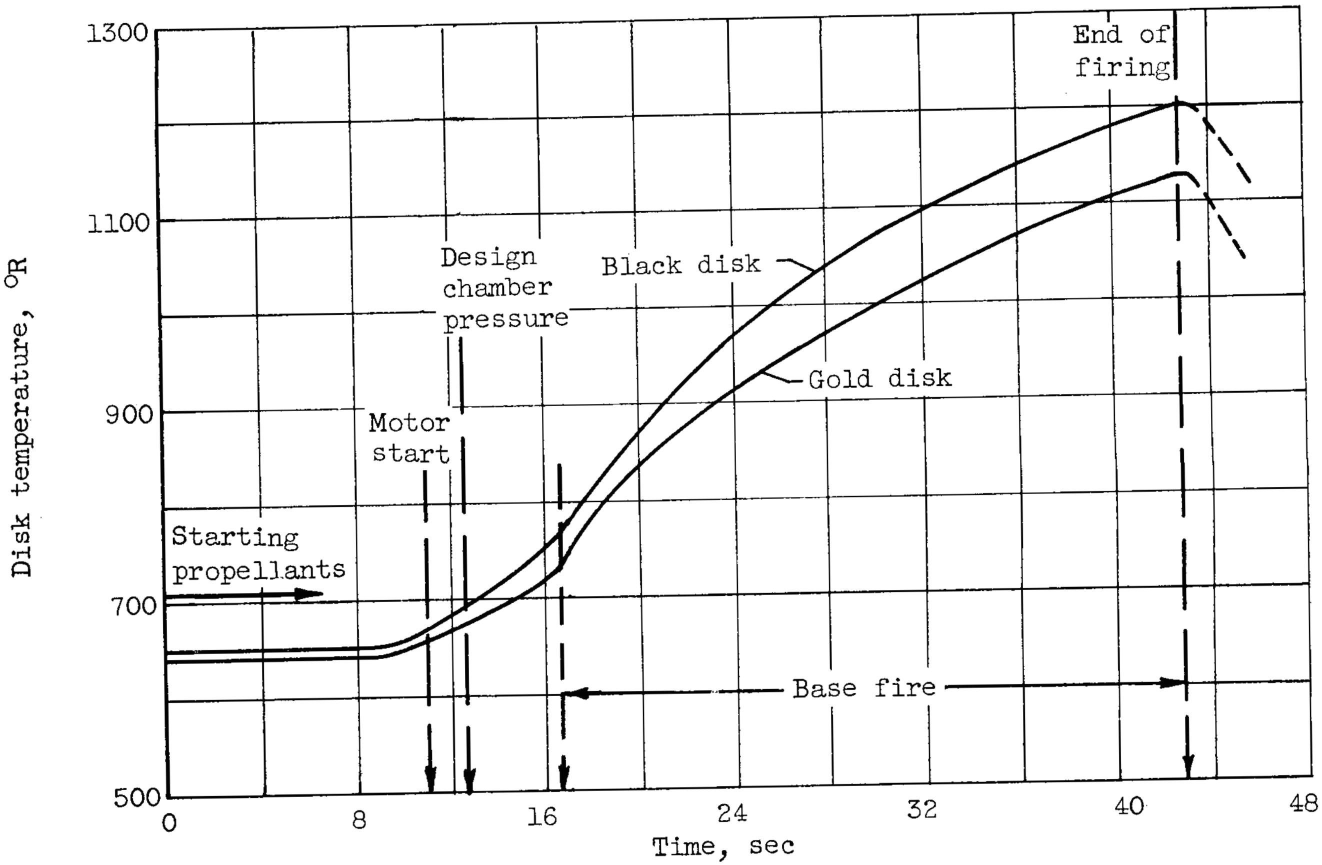

Figure 9. - Calorimeter disk temperatures during rocket firing with base fire.

[redacted]

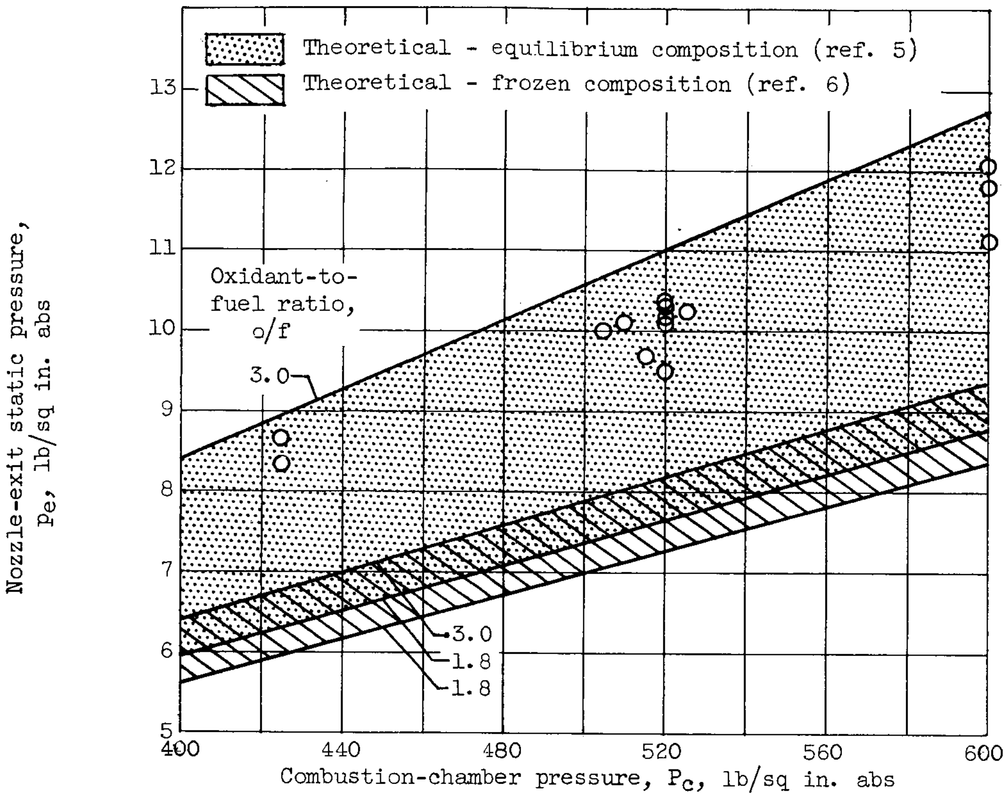

(a) Nozzle-exit static pressure.

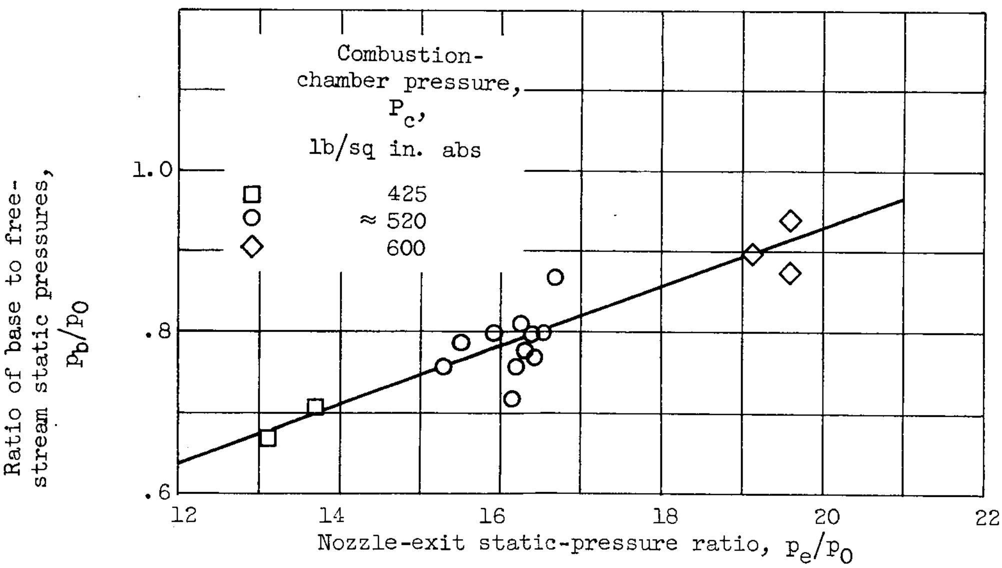

(b) Model base pressure.

Figure 10. - Comparison of combustion-chamber pressure, nozzle-exit static pressure, and base pressure.

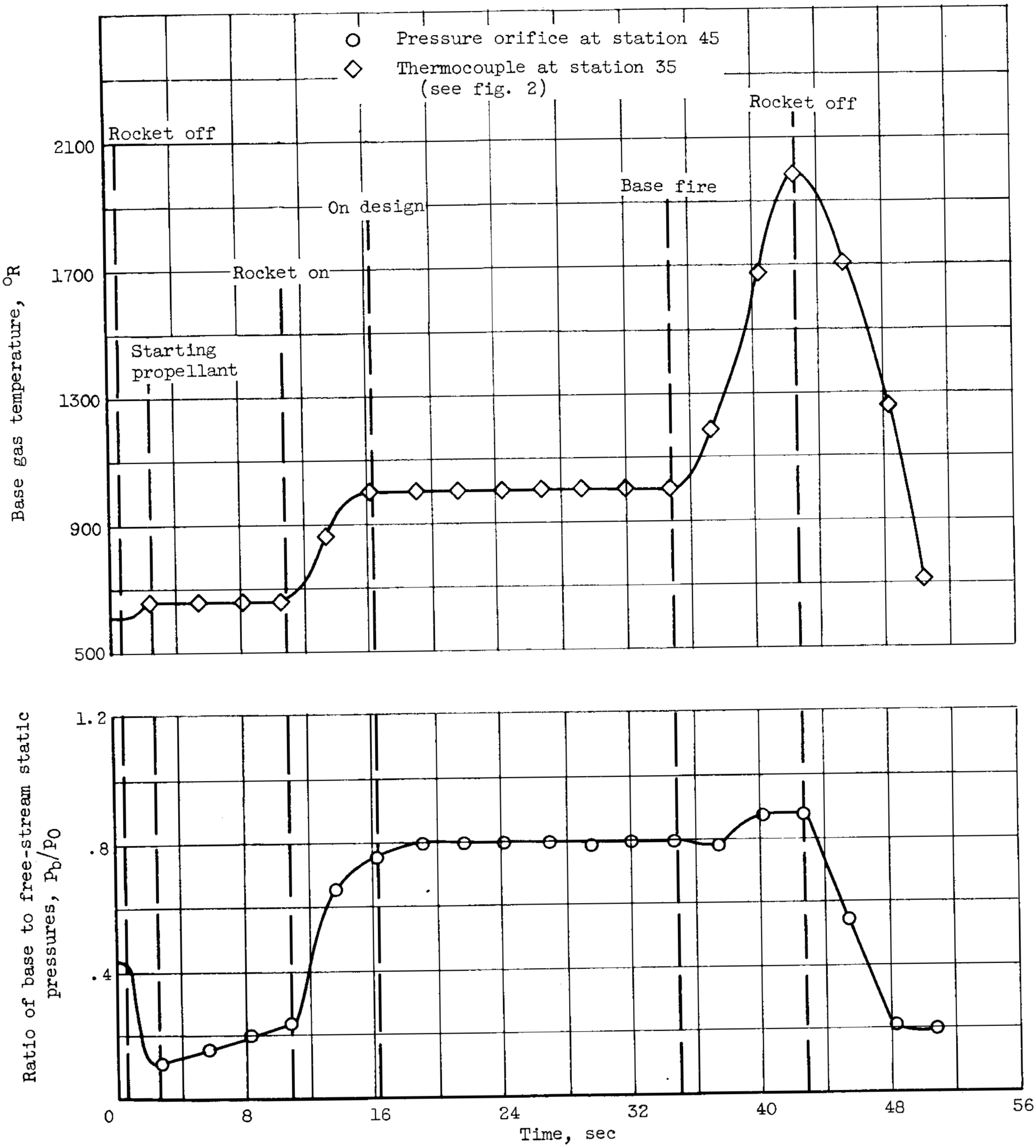

Figure 11. - Base pressures and gas temperature during a firing with base fire. Combustion-chamber pressure, 525 pounds per square inch absolute; oxidant-to-fuel ratio, 2.3.

[redacted]